# Discrete eigenmodes of filamentation instability in the presence of a $q$-nonextensive distribution

M. Hashemzadeh*
*Faculty of Physics, Shahrood University of Technology, Shahrood, Semnan Province, Iran*

(Received 17 July 2018; revised manuscript received 23 November 2019; published 6 January 2020)

Discrete eigenmodes of the filamentation instability in a weakly ionized current-driven plasma in the presence of a $q$-nonextensive electron velocity distribution is investigated. Considering the kinetic theory, Bhatnagar-Gross-Krook collision model, and Lorentz transformation relations, the generalized longitudinal and transverse dielectric permittivities are obtained. Taking into account the long-wavelength limit and diffusion frequency limit, the dispersion relations are obtained. Using the approximation of geometrical optics and linear inhomogeneity of the plasma, the real and imaginary parts of the frequency are discussed in these limits. It is shown that in the long-wavelength limit, when the normalized electron velocity is increased the growth rate of the instability increases. However, when the collision frequency is increased the growth rate of the filamentation instability decreases. In the diffusion frequency limit, results indicate that the effects of the electron velocity and $q$-nonextensive parameter on the growth rate of the instability are similar. Finally, it is found that when the collision frequency is increased the growth rate of the instability increases in the presence of a $q$-nonextensive distribution.

DOI: 10.1103/PhysRevE.101.013202

## I. INTRODUCTION

Current filamentation instability is an important subject in laser-plasma and beam-plasma interactions that was investigated more than 50 years ago [1–3]. This instability has attracted much attention due to its variety of applications including inertial confinement fusion [4], charged particle acceleration [5,6], cosmic rays, and shock waves [7]. The filamentation instability occurs when a perturbation propagates normal to the beam propagation direction. This mode is sometimes called the transverse mode. However, for two-stream instability (longitudinal mode), the perturbations propagate parallel to the direction of the stream. In general, when the perturbations propagate in the oblique direction, both two-stream and filamentation instabilities can get excited within the plasma [8]. However, as mentioned above, the filamentation instability is the current-driven one. This instability usually contains two beams: the injected electron beam and the induced counter-streaming beam. Note that the injected electron beam induces charges and currents in the plasma which neutralize the charge and current of the beam. Therefore, the total current density is approximately 0, i.e., $e(N_b u_b - N_p u_p) \approx 0$, where $N_b$ ($N_p$) and $u_b$ ($u_p$) are the beam density (plasma density) and beam velocity (plasma velocity), respectively. Thus, $u_p \approx u_b N_b/N_p$. Assuming that the plasma density $N_p$ greatly exceeds the electron beam density $N_b$, one can neglect the plasma velocity $u_p$ and the calculation is valid [9]. The process of the filamentation instability can be described as follows: At the beginning in some regions the amplitude of the perturbation increases with the electron current and the main filaments are produced. As time passes, the adjacent microfilaments join to the main filaments and the formation of the main filaments becomes complete. At later times, the magnetic pinch force increases the current density of these filaments, which leads to the enhancement of the amplitude of the magnetic field. At the same time, the charge separation between bunched electrons and immobile background ions can create an electrostatic field. This electric field inhibits the growth rate of the filaments, and consequently the growth of the filaments is suppressed. The suppression of filaments occurs at a time known as the saturation time [10].

Filamentation instability has been investigated by many authors theoretically, experimentally, and by computer simulations. Filamentation and magnetic-field generation by charged particle beams in laser-produced plasmas have been investigated by Aliev *et al.* [11]. They found that the kinetic instability caused by the anomalous skin effect in plasma penetrated by a fast electron beam may be responsible for the formation of magnetic fields and current filaments in the plasma corona. Califano *et al.* [12] have studied the linear and nonlinear evolution of the electromagnetic beam-plasma instability in a collisionless inhomogeneous plasma by using a set of two fluid electron equations in the nonrelativistic and relativistic regimes. They concluded that their results can be used as a signature of the physical mechanism in the analysis of the numerical and experimental results of the laser-plasma interaction. Using theoretical methods, eigenmodes and growth rates of relativistic current filamentation instability in a collisional plasma have been explored by Honda [13]. He found that in the stronger collisional regime, the growing oscillatory mode tends to be dominant for all wavelengths. In the collisionless limit, these modes vanish, while maintaining another purely growing mode that exactly coincides with a standard relativistic Weibel mode. In addition to this work, Mohammadhosseini *et al.* [14] have explored the spatial and temporal evolution of filamentation instability

*hashemzade@gmail.com

 

in a current-carrying plasma in the nonlinear regime. They have shown that as time passes, the profile of the electric and magnetic fields changes from a sinusoidal shape to a sawtooth one and the electron density distribution becomes very steep.

However, most of the aforementioned works have studied the filamentation or Weibel instabilities in the presence of a Maxwellian distribution function. Some years ago, multifractal concepts encouraged Renyi [15] and then Tsallis [16] to propose a $q$-nonextensive distribution for nonequilibrium environments (non-Maxwellian distribution). Non-Maxwellian distributions have been examined by some observations done in the Earth's bow shock [17], in the upper ionosphere of Mars [18], in the vicinity of the Moon [19], and in the magnetosphere of Jupiter and Saturn [20,21]. This $q$-nonextensive distribution can be used for systems with long-range interactions, such as plasmas and gravitational systems [22]. Liu *et al.* [23] in 1994 provided strong evidence of the existence of non-Maxwellian velocity distributions in a specific plasma experiment, where low-pressure argon was exposed to pulsed discharges. During the afterglow, measurements of the inverse bremsstrahlung of intense microwaves were performed. Tsallis and Souza [24] showed in 1997 that their afterglow experimental data can equally well be fitted with a $q$-nonextensive distribution for $q \geqslant 1$. They concluded that the $q$ parameter depends on the microwave power. Non-Maxwellian electron distribution functions in glow discharges (current, 5–50 mA; pressure, 200–1000 Pa) were derived from the intensities of Ar and He spectral lines and $N_2$ molecular bands with different excitation thresholds. Experimental observations of a magnetospheric fractal accelerator of charged particles [25–29] illustrated that the $q$-nonextensive parameter is $2.49 \pm 0.07$, $2.15 \pm 0.07$, and $2.49 \pm 0.05$. Moreover, the $q$ parameter obtained for cosmic rays was $1.44 \pm 0.05$ [30]. Dispersion relations for electrostatic plane-wave propagation in a collisionless thermal plasma have been discussed in the context of nonextensive statistics by Lima *et al.* [31]. It was shown that the experimental results point to a class of Tsallis's velocity distribution described by a nonextensive $q$ parameter smaller than unity. Qiu and Liu [32] have obtained the Weibel instability growth rate in a collisionless, unbounded, unmagnetized plasma modeled by a nonextensive electron distribution function with different $q$ parameters. They found that the nonextensive nature of the electron distribution has an important effect on the Weibel instability. The filamentation and ion acoustic instabilities of nonextensive current-driven plasma in the ion acoustic frequency range have been studied by Khorashadizadeh *et al.* [33] using the Lorentz transformation formulas. Moreover, the evolution of filamentation instability in a current-driven dusty plasma with a nonextensive distribution has been investigated by Niknam *et al.* [34] in the dust acoustic frequency range. Hashemzadeh [35] has explored the ion-acoustic and Buneman instabilities in a current-carrying plasma taking into account the collisional effects and $q$-nonextensive distribution function.

Most of the aforementioned works have investigated the filamentation or Weibel instability in homogeneous plasma. Although some authors have studied the instabilities in inhomogeneous plasma [36–39], the filamentation instability in inhomogeneous bounded plasma in the presence of a $q$-nonextensive distribution function has not been explored. In this work, it is assumed that a plasma slab is located in the $x$ direction ($0 \leqslant x \leqslant L$). The plasma is supposed to be collisional, unmagnetized, and inhomogeneous with linear inhomogeneity. It is important to note that, in practice, the plasma produced in the progress of reentry or entry flights is inhomogeneous [40]. Moreover, the plasma corona which forms around an initially solid target under laser irradiation is presented by an inhomogeneous plasma model [41]. Electrons have a $q$-nonextensive distribution function, while ions are at rest because they are very massive. Considering the Bhatnagar-Gross-Krook (BGK) collision model, $q$-nonextensive velocity distribution, and kinetic equation, a generalized $q$ dielectric permittivity is obtained. The dispersion relations of the filamentation instability in the diffusion frequency limit and long-wavelength limit are obtained. Results show that in the long-wavelength limit, when the normalized electron velocity is increased, both the real and the imaginary parts of the frequency increase. Opposite to this behavior, when the normalized collision frequency is increased, the real and imaginary parts of the frequency decrease. In the diffusion frequency limit, for normalized electron velocities less than 0.36, the system is stable, while for values greater than this the plasma system is unstable. This behavior is also seen for different values of the $q_e$ parameter. It is also indicated that the normalized collision frequency enhances the growth rate of the instability.

This work is organized in five sections. In Sec. II, the basic equations are presented. Using the kinetic theory, BGK collision model, and $q$-nonextensive velocity distribution, the generalized dielectric permittivity and, consequently, the $q$ dispersion relation are obtained. In Sec. III, the dispersion relations of the filamentation instability for the long-wavelength and diffusion frequency limits are obtained. The effects of collision, the electron drift velocity, and the $q$-nonextensive parameter in these limits are discussed in Sec. IV. Finally in Sec. V, a summary and conclusions are given.

## II. BASIC EQUATIONS

Consider a weakly ionized inhomogeneous unmagnetized multicomponent plasma consisting of neutrals ($n$), ions ($i$), and electrons ($e$) with electrons moving in the $z$ direction. Ions are assumed to be immobile because they are very massive. In this plasma, electrons obey the $q$-nonextensive distribution function. In the $q$-nonextensive framework, the three-dimensional momentum distribution function can be expressed as [10,35]

$$f_{0e}(q_e, \mathbf{p}, T_e) = B_{q_e} N_e(x) \left[ 1 - (q_e - 1) \frac{\mathbf{p}^2}{m_e^2 v_{T_e}^2} \right]^{\frac{2-q_e}{q_e-1}}, \quad (1)$$

where $B_{q_e}$ is the normalized constant

$$B_{q_e} = \frac{\Gamma\left(\frac{1}{1-q_e}\right)(1-q_e)^{1/2}}{\Gamma\left(\frac{1}{1-q_e} - \frac{1}{2}\right)} \left( \frac{1}{\pi v_{T_e}^2} \right)^{3/2}, \quad -1 < q_e < 1, \quad (2)$$

and

$$B_{q_e}=\left(\frac{1+q_e}{2}\right)\frac{\Gamma\left(\frac{1}{q_e-1}+\frac{1}{2}\right)(q_e-1)^{1/2}}{\Gamma\left(\frac{1}{q_e-1}\right)}\left(\frac{1}{\pi v_{T_e}^2}\right)^{3/2},\quad q_e>1, \tag{3}$$

where $q_e$ is the strength of the nonextensivity of electrons, $\Gamma$ is the standard gamma function, $v_{T_e}=(\frac{2T_e}{m_e})^{1/2}$ is the electron thermal velocity, and $N_e(x)$ is the inhomogeneous (initial) electron density.

The $q$-nonextensive electron density distribution is normalized to unity:

$$\int f_{0e}(q,\mathbf{p},T_e)d^3\mathbf{v}=1. \tag{4}$$

It is noteworthy that in the range $q_e<-1$, Eq. (1) is not normalizable. In the range $0<q_e<1$, the distribution function has a power-law tail at high energies, and in the range $q_e>1$, there is a thermal cutoff of this distribution function, $v_{\max,e}=v_{T_e}/(q_e-1)^{1/2}$. As expected, in the limit $q_e\to 1$, Eq. (1) is reduced to the well-known Maxwell-Boltzman distribution function. It is important to note that the constant $T_e$ in Eqs. (1)-(3) is a formal constant with an energy dimension and the effective electron temperature, $T_{\rm eff}$, represents the physical property of the system obtained as [42]

$$\begin{aligned}&T_{\rm eff}(q_e,T_e)\\&=\frac{1}{m_e^4N_e(x)}\begin{cases}\int_{-\infty}^{\infty}\mathbf{p}^2f_{0e}(q_e,\mathbf{p},T_e)d^3\mathbf{p}, & \frac{1}{3}<q_e<1,\\ int_{-v_{\max,e}}^{v_{\max,e}}\mathbf{p}^2f_{0e}(q_e,\mathbf{p},T_e)d^3\mathbf{p}, & q_e>1,\end{cases}\\&=-\frac{\Gamma\left(-\frac{3}{2}+\frac{1}{q_e-1}\right)}{\Gamma\left(\frac{1+q_e}{2-2q_e}\right)}\frac{T_e}{q_e-1},\end{aligned} \tag{5}$$

and $v_{\max,e}$ was presented above. It is easy to show that in the limit $q_e\to 1$, the effective electron temperature goes to $T_e$.

On the other hand, in the beginning, it is assumed that the plasma is inhomogeneous, collisional, unmagnetized, and at $q$-nonextensive equilibrium. When the plasma deviates slightly from the initial state, the electron distribution function can be expressed as

$$f_e(\mathbf{p},\mathbf{r},t)=f_{0e}(\mathbf{p},\mathbf{r})+\delta f_{1e}(\mathbf{p},\mathbf{r},t),\quad \delta f_{1e}\ll f_{0e}, \tag{6}$$

where $\delta f_{1e}$ is the perturbation about $f_{0e}$. In addition, it is assumed that the perturbation is in the form $\exp(i(\mathbf{k}\cdot\mathbf{r}-\omega t))$. Moreover, in order to investigate the collisional effect in plasmas the Fokker-Planck equation, or at least a Fokker-Planck-type equation, can be useful. But as we know, this equation is very complex and the results are complicated. Instead, another simple model used in weakly ionized plasmas and known as the Krook model or Bhatnagar-Gross-Krook collisional model can be applied. The standard formula of the Boltzmann kinetic equation for electrons with the BGK collision term is [9,10]

$$\begin{aligned}&\frac{\partial\delta f_{1e}}{\partial t}+\mathbf{v}\cdot\frac{\partial\delta f_{1e}}{\partial\mathbf{r}}+e\mathbf{E}\cdot\frac{\partial f_{0e}}{\partial\mathbf{p}}\\&\quad=-\nu_{en}(\delta f_{1e}-f_{0e}\int\delta f_{1e}d\mathbf{p}),\end{aligned} \tag{7}$$

where $\mathbf{E}(\mathbf{r},t)$ is the perturbed electric field, $e$ is the charge of electrons, $\mathbf{v}$ is the velocity of electrons, and $\nu_{\rm en}$ is the electron-neutral collision frequency. The left-hand side of Eq. (7) is the total time derivative of the distribution function and the right-hand side is responsible for the elastic collisions. On the right-hand side, the following assumptions are considered: (i) Only binary collisions occur in the plasma; (ii) the distribution function is slowly varying; and (iii) the term on the right-hand side is consistent with the energy, momentum, and particle number conservation laws [43]. It is important to note that in weakly ionized plasmas, the collision between charged particles and neutrals is considered, while electron-electron and ion-ion collisions can be neglected. For example, in the E region at altitudes 91, 96, 101, 109, 117, and 125 km and the F region at altitude 278 km the dominant collision frequency is the ion-neutral collision frequency [44]. Moreover, in radio-frequency glow discharges at temperature 300 K and pressure 1 T, the ion-neutral collision frequency is 7.84–15.5 MHz. However, in these plasmas filamentation instability can exist [45]. It is noteworthy that the perturbed electric field is assumed to be in the form $\exp(i(\mathbf{k}\cdot\mathbf{r}-\omega t))$. In addition, the frequency $\omega$ presented above is known as the "eigenmodes" that are excited in the filamentation instability. The charge and current densities in plasma are related to $\delta f_{1e}$ and $\mathbf{E}(\mathbf{r},t)$ by

$$\rho=e\int\delta f_{1e}d\mathbf{p}, \tag{8}$$

$$J_i=\sigma_{ij}E_j=e\int v_if_{1e}d\mathbf{p}, \tag{9}$$

where $\sigma_{ij}$ is the conductivity tensor and is related to the dielectric permittivity tensor $\varepsilon_{ij}$ by

$$\varepsilon_{ij}=\delta_{ij}+\frac{4\pi i}{\omega}\sigma_{ij}, \tag{10}$$

where $\delta_{ij}$ is the Kronecker delta function. In isotropic plasmas, the dielectric permittivity tensor can be obtained as [9]

$$\varepsilon_{ij}(\omega,\mathbf{k})=\left(\delta_{ij}-\frac{k_ik_j}{k^2}\right)\varepsilon^{\rm tr}(\omega,\mathbf{k})+\frac{k_ik_j}{k^2}\varepsilon^{\rm lo}(\omega,\mathbf{k}), \tag{11}$$

where $\varepsilon^{\rm tr}(\omega,\mathbf{k})$ and $\varepsilon^{\rm lo}(\omega,\mathbf{k})$ are the transverse and longitudinal dielectric permittivities, respectively. Moreover, the continuity equation is

$$\frac{\partial\rho}{\partial t}+\nabla\cdot J=0. \tag{12}$$

Using Eqs. (1) and (7)– (12), the longitudinal dielectric permittivity can be obtained as

$$\varepsilon^{\rm lo}=1+\frac{4\pi e^2}{\omega}\frac{\int\frac{v_\parallel\frac{\partial f_{0e}(p_\parallel)}{\partial p_\parallel}}{\omega+i\nu_{\rm en}-kv_\parallel}d\mathbf{p}}{1-\frac{i\nu_{\rm en}k}{\omega}\int\frac{v_\parallel f_{0e}(p_\parallel)}{\omega+i\nu_{\rm en}-kv_\parallel}d\mathbf{p}}, \tag{13}$$

where

$$\begin{aligned}f_{0e}(p_\parallel)&=2\pi\int f_{0e}(\mathbf{p})dp_\perp\\&=\pi v_{T_e}^2B_{q_e}N_e(x)\left[1-(q_e-1)\frac{p_\parallel^2}{m_e^2v_{T_e}^2}\right]^{\frac{1}{q_e-1}}.\end{aligned} \tag{14}$$

In Eqs. (13) and (14), $v_\parallel$ ($p_\parallel$) and $v_\perp$ ($p_\perp$) are the velocity (momentum) components parallel and perpendicular to the wave vector $\mathbf{k}$, respectively. Similarly to the longitudinal case, the transverse dielectric permittivity can be obtained as

$$\varepsilon^{\mathrm{tr}} = 1 + \frac{2\pi e^2}{\omega}\int v_\perp \cdot \frac{\partial f_{0e}}{\partial p_\perp}\frac{d\mathbf{p}}{\omega + i\nu_{\mathrm{en}} - kv_\parallel}. \tag{15}$$

Substituting Eqs. (1) and (14) into Eqs. (13) and (15), the longitudinal and transverse dielectric permittivities in a magnetic-field-free plasma are as follows:

$$\varepsilon^{\mathrm{lo}}(\omega,k) = 1 + \frac{2\omega_{p_e}^2(x)}{k^2 v_{T_e}^2}\frac{\frac{q_e+1}{2} + \left(\frac{\omega+i\nu_{\mathrm{en}}}{kv_{T_e}}\right)Z_{q_e}^{(1)}\left(\frac{\omega+i\nu_{\mathrm{en}}}{kv_{T_e}}\right)}{1 + \frac{i\nu_{\mathrm{en}}}{kv_{T_e}}Z_{q_e}^{(2)}\left(\frac{\omega+i\nu_{\mathrm{en}}}{kv_{T_e}}\right)}, \tag{16}$$

$$\varepsilon^{\mathrm{en}}(\omega,k) = 1 - \frac{\omega_{p_e}^2(x)}{\omega(\omega+i\nu_{\mathrm{en}})}Z_{q_e}^{(3)}\left(\frac{\omega+i\nu_{\mathrm{en}}}{kv_{T_e}}\right), \tag{17}$$

where $\omega_{p_e}(x) = (4\pi N_e(x)e^2/m_e)^{1/2}$ and $Z_{q_e}^{(1)}(y)$, $Z_{q_e}^{(2)}(y)$, and $Z_{q_e}^{(3)}(y)$ are the generalized $q$ dispersion functions defined as

$$\begin{aligned}
Z_{q_e}^{(1)}(y) &= B'_{q_e} v_{T_e}\int_{-\infty}^{\infty}\frac{[1-(q_e-1)u^2]^{\frac{1}{q_e-1}-1}}{u-y}du \\
&= PB'_{q_e} v_{T_e}\int_{-\infty}^{\infty}\frac{[1-(q_e-1)u^2]^{\frac{1}{q_e-1}-1}}{u-y}du \\
&\quad + i\pi B'_{q_e} v_{T_e}[1-(q_e-1)y^2]^{\frac{1}{q_e-1}-1}, \\
Z_{q_e}^{(2)}(y) &= B'_{q_e} v_{T_e}\int_{-\infty}^{\infty}\frac{[1-(q_e-1)u^2]^{\frac{1}{q_e-1}}}{u-y}du \\
&= PB'_{q_e} v_{T_e}\int_{-\infty}^{\infty}\frac{[1-(q_e-1)u^2]^{\frac{1}{q_e-1}}}{u-y}du \\
&\quad + i\pi B'_{q_e} v_{T_e}[1-(q_e-1)y^2]^{\frac{1}{q_e-1}}, \\
Z_{q_e}^{(3)}(2y) &= B'_{q_e} v_{T_e} y\int_{-\infty}^{\infty}\frac{[1-(q_e-1)u^2]^{\frac{1}{q_e-1}}}{y-u}du \\
&= PB'_{q_e} v_{T_e} y\int_{-\infty}^{\infty}\frac{[1-(q_e-1)u^2]^{\frac{1}{q_e-1}}}{y-u}du \\
&\quad + i\pi B'_{q_e} v_{T_e} y[1-(q_e-1)y^2]^{\frac{1}{q_e-1}},
\end{aligned} \tag{18}$$

where $B'_{q_e} = \pi v_{T_e}^2 B_{q_e}$ and $P$ is the principal value. The first term on the right-hand side of Eqs. (18) (the principal value term) is responsible for the nonresonant electrons, while the second term is responsible for the resonant electrons contributing to the Landau damping [46]. As mentioned in Sec. I, the filamentation instability arises in a current-driven plasma in which the electrons move thorough a stationary ion background. In this case, Eqs. (16)–(18) should be modified. Using the Lorentz transformations in the nonrelativistic regime,

$$\begin{aligned}
\omega' &= \omega - \mathbf{k}\cdot\mathbf{u}_e,\ \xi_{ij}(\mathbf{u}_e) = \delta_{ij} + \frac{k_j u_{ie}}{\omega - \mathbf{k}\cdot\mathbf{u}_e}, \\
\eta_{ij}(\mathbf{u}_e) &= \frac{\omega - \mathbf{k}\cdot\mathbf{u}}{\omega}\delta_{ij} + \frac{k_i u_{je}}{\omega},
\end{aligned} \tag{19}$$

where $\mathbf{u}_e$ is the electron velocity. Therefore, the dielectric permittivity tensor in the presence of moving electrons is obtained,

$$\varepsilon_{ij}(\omega,\mathbf{k}) = \delta_{ij} + \sum_{\alpha,\beta}\frac{\omega'}{\omega}\xi_{i\alpha}(\mathbf{u}_e)[\varepsilon_{\alpha\beta}(\omega',\mathbf{k}-\delta_{\alpha\beta})]\eta_{\beta j}(\mathbf{u}_e), \tag{20}$$

where $\varepsilon_{\alpha\beta}(\omega',\mathbf{k})$ is the dielectric permittivity in its respective moving frame. Taking into account the longitudinal and transverse dielectric permittivities and using Eqs. (11), (19), and (20), the dielectric permittivity tensor is presented as

$$\begin{aligned}
\varepsilon_{ij}(\omega,\mathbf{k}) = \left(\frac{\omega'}{\omega}\right)^2\Bigg[&\left(\delta_{ij} - \frac{k_i k_j}{k^2}\right)(\varepsilon^{\mathrm{tr}}(\omega',k)-1) \\
&+ \left\{\frac{k_i k_j}{k^2} + \frac{u_i k_j + u_j k_i}{\omega'} + \frac{u_i u_j k^2}{\omega'^2}\right\} \\
&\times (\varepsilon^{\mathrm{lo}}(\omega',k)-1)\Bigg].
\end{aligned} \tag{21}$$

Considering Eq. (21) and taking into account the general dispersion equation

$$\left|k^2\delta_{ij} - k_i k_j - \frac{\omega^2}{c^2}\varepsilon_{ij}(\omega,\mathbf{k})\right| = 0, \tag{22}$$

the filamentation instability in a current-driven plasma can be investigated.

## III. FILAMENTATION INSTABILITY

In this section, the current-driven filamentation instability in an inhomogeneous, unmagnetized, nonextensive plasma is studied in the long-wavelength limit and diffusion frequency limit. The wave vector is assumed to be in the $x$ direction, $\mathbf{k} = (k,0,0)$, and electrons move at a drift velocity along the $z$ axis, $\mathbf{u}_e = (0,0,u)$. Therefore, the propagation is perpendicular to the electron velocity, $\mathbf{k}\cdot\mathbf{u}_e = 0$. It is also supposed that the frequency of the wave is low, $\omega \ll kc, \omega_{p_i}, \omega_{p_e}$. In addition, the plasma is in the diffusion frequency region, i.e., $\nu_{\mathrm{in}}, kv_{T_i} \ll \omega \ll kv_{T_e} \ll \nu_{\mathrm{en}}$. Under these conditions, the longitudinal and transverse dielectric permittivities [Eqs. (16) and (17)] become

$$\varepsilon^{\mathrm{lo}}(\omega,k) = 1 - \frac{\omega_{p_i}^2}{\omega^2} - \frac{\omega_{p_e}^2}{i\omega\nu_{\mathrm{en}} - \frac{2k^2 v_{T_e}^2}{3q_e-1}}, \tag{23}$$

$$\varepsilon^{\mathrm{tr}}(\omega,k) = 1 - \frac{\omega_{p_i}^2}{\omega^2} + i\frac{\omega_{p_e}^2}{\omega\nu_{\mathrm{en}}}. \tag{24}$$

In the above equations, it is supposed that ions oscillate around their initial positions. Considering the conditions presented above and using Eqs. (23) and (24), the general dispersion relation is reduced to

$$\varepsilon_{11}(\omega,k)\left(\frac{c^2k^2}{\omega^2} - \varepsilon_{33}(\omega,k)\right) + \varepsilon_{13}^2(\omega,k)) = 0, \tag{25}$$

where

$$\varepsilon_{11}(\omega,k)=1-\frac{\omega_{p_i}^2}{\omega^2}-\frac{\omega_{p_e}^2}{i\omega\nu_{\rm en}-\frac{2k^2v_{T_e}^2}{3q_e-1}}, \tag{26}$$

$$\varepsilon_{13}(\omega,k)=-\frac{ku\omega_{p_e}^2}{\omega\left(i\omega\nu_{\rm en}-\frac{2k^2v_{T_e}^2}{3q_e-1}\right)}-\frac{uk\omega_{p_i}^2}{\omega^3}, \tag{27}$$

$$\varepsilon_{33}(\omega,k)=1+\frac{\omega_{p_e}^2}{\omega\nu_{\rm en}}-\frac{\omega_{p_i}^2}{\omega^2}-\frac{k^2u^2\omega_{p_e}^2}{\omega^2\left(i\omega\nu_{\rm en}-\frac{2k^2v_{T_e}^2}{3q_e-1}\right)}. \tag{28}$$

This dispersion relation is solved in two limits, the long-wavelength limit and diffusion frequency limit. In the long-wavelength limit and under the condition $(3q_e-1)\omega\nu_{\rm en}\gg 2k^2v_{T_e}^2$, Eq. (25) is simplified to

$$\left(-i\omega_{p_e}^2(x)u^2+\omega\nu_{\rm en}c^2\right)k^2+\omega\nu_{\rm en}\omega_{p_i}^2=0. \tag{29}$$

In the diffusion frequency limit, $(3q_e-1)\omega\nu_{\rm en}\ll 2k^2v_{T_e}^2$, Eq. (25) is reduced to

$$k^2c^2+\omega_{p_i}^2-i\frac{\omega_{p_e}^2(x)\omega}{\nu_{\rm en}}-\frac{\omega_{p_e}^2(x)u^2(3q_e-1)}{2v_{T_e}^2}=0. \tag{30}$$

Equations (29) and (30) are the eikonal equations for an inhomogeneous plasma with spatial variation. However, the eigenmodes of the filamentation instability can be obtained from these equations.

## IV. APPROXIMATION OF GEOMETRICAL OPTICS FOR INHOMOGENEOUS PLASMA AND QUANTIZATION RULES

In Sec. III, the eikonal equations for an inhomogeneous plasma with linear variation in two different limits have been obtained. The plasma is assumed to be in a slab 0–$L$ along the $x$-axis region. Plasma is supposed to be weakly inhomogeneous on the scale of the wavelength of the electromagnetic oscillations. This means that the wavelength $\lambda$ is much smaller than the characteristic length of the inhomogeneity, i.e., $\lambda\ll L$. In this case, the dispersion relation or eigenmodes can be obtained as [9]

$$\int_0^L k_x(\omega,x)dx=n\pi, \tag{31}$$

where $n$ is an arbitrary integer number. Moreover, the inhomogeneity of the electron density expressed above is [39]

$$N_e(x)=\frac{N_{e0}x}{L}, \tag{32}$$

where $N_{e0}$ is the initial electron density in the absence of inhomogeneity. It is noteworthy that according to Eq. (32), the inhomogeneity of the electron density is linear, which is applicable for $q>1/3$. In the homogeneous plasma the background electron density is $N_{e0}$. These are two separated models. However, one can couple these models as $N_e=N_{e0}+N_{e1}x/L$ and obtain the growth rate of the instability again. In the long-wavelength limit, the wave number has been obtained

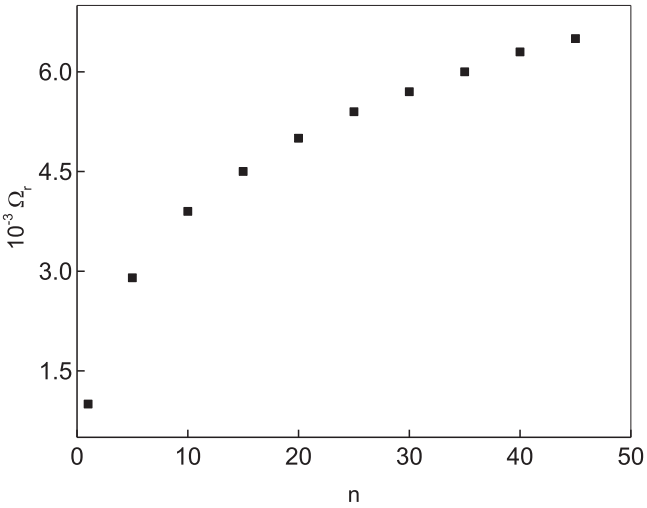


FIG. 1. Real part of the frequency $\Omega_r$ for different values of the $n$ parameter.

from Eq. (29) as

$$k_x(\omega,x)=\frac{\sqrt{\omega\nu_{\rm en}}\omega_{p_i}}{\sqrt{iu^2\omega_{p_{e0}}^2\frac{x}{L}-\omega\nu_{\rm en}c^2}}, \tag{33}$$

where $\omega_{p_{e0}}=(4\pi N_{e0}e^2/m_e)^{1/2}$. Substituting Eq. (33) into Eq. (31), we have

$$-\frac{2iL\omega_{p_i}\sqrt{\omega\nu_{\rm en}}}{u^2\omega_{p_{e0}}^2}\left[\sqrt{iu^2\omega_{p_{e0}}^2-\omega\nu_{\rm en}c^2}-\sqrt{-\omega\nu_{\rm en}c^2}\right]=n\pi. \tag{34}$$

Using the dimensionless parameters, $\nu_{\rm en}/\omega_{p_{e0}}=\nu$, $\omega/\omega_{p_{e0}}=\Omega$, $u/c=U$, $\omega_{p_i}/\omega_{p_{e0}}=\Omega_i$, and $L\omega_{p_{e0}}/c=L'$, Eq. (34) becomes

$$-\frac{2iL'\Omega_i\sqrt{\Omega\nu}}{U^2}\left[\sqrt{iU^2-\Omega\nu}-\sqrt{-\Omega\nu}\right]=n\pi. \tag{35}$$

Using numerical techniques, i.e., the Newton-Raphson method, the real $\Omega_r$ and imaginary $\Gamma$ parts of the frequency can be obtained. In Fig. 1 the $\Omega_r$ parameter for different values of $n$ is plotted. The parameters used in this figure are $U=0.05$, $\nu=0.5$, $L'=10$, and $\Omega_i=0.025$. The imaginary part of the frequency $\Gamma$ for all $n$ parameters is the same, 0.005. It is clear in this figure that when the $n$ parameter is increased, $\Omega_r$ increases. In addition, a positive value of the $\Gamma$ parameter indicates that the system is unstable. Comparing the results obtained in Fig. 1 vs Eq. (18) in Ref. [10], one can easily find that for homogeneous plasma the frequency is purely imaginary, while for the inhomogeneous case the frequency contains both real and imaginary parts. It is important to note that when the plasma system is bounded in a certain region, standing waves can be formed, and consequently, it is expected that the frequency has a discrete value. In Fig. 2, $\Omega_r$ and $\Gamma$ for different values of the normalized electron velocity are drawn. Parameters used in this figure are $n=10$, $\nu=0.25$, $L'=10$, and $\Omega_i=0.025$. $k'=ck/\omega_{p_{e0}}$ is also 0.1 for the homogeneous case [see Eq. (29)]. In addition, the growth rate has been obtained in the presence of inhomogeneity and homogeneity of the electron density. It is important to note that $\Omega_r$ in the homogeneous case is 0. It is obvious

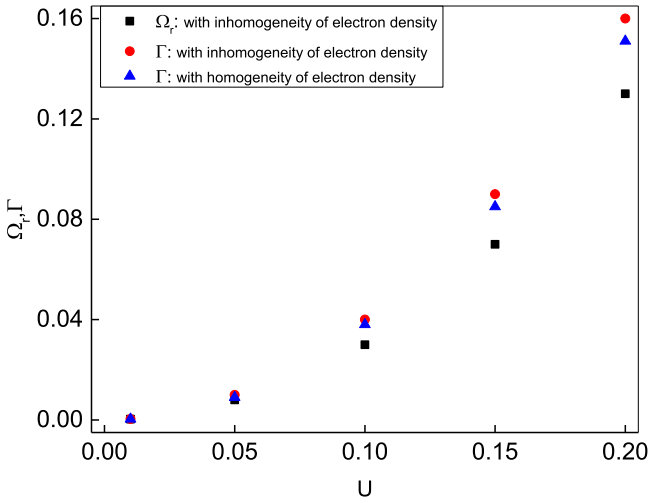


FIG. 2. Real $\Omega_r$ and imaginary $\Gamma$ parts of the frequency for different values of the $U$ parameter.

in this figure that when the electron velocity is increased, the growth rate of the instability $\Gamma$ increases. Moreover, $\Omega_r$ increases upon increasing the $U$ parameter. As we know, the filamentation instability is a current-driven instability in which the energy can exchange between (electron or ion) beam and plasma. When the electron velocity is increased, the energy of the beam increases, and consequently more energy can be transferred to the plasma wave and its amplitude increases. It is noteworthy that the plasma wave is proportional to $\exp[i(\mathbf{k}\cdot\mathbf{r}-\omega t)]$. Furthermore, Fig. 2 indicates that the effect of inhomogeneity of the electron density on the $\Gamma$ parameter is the same as in the homogeneity case. The effect of the normalized collision frequency on the real and imaginary parts of the frequency is depicted in Fig. 3. In this figure $U = 0.05$ and other parameters are similar to those in Fig. 2. One can see in Fig. 3 that when the collision frequency is increased, both $\Omega_r$ and $\Gamma$ decrease. This means that the collision frequency can stabilize the plasma system.

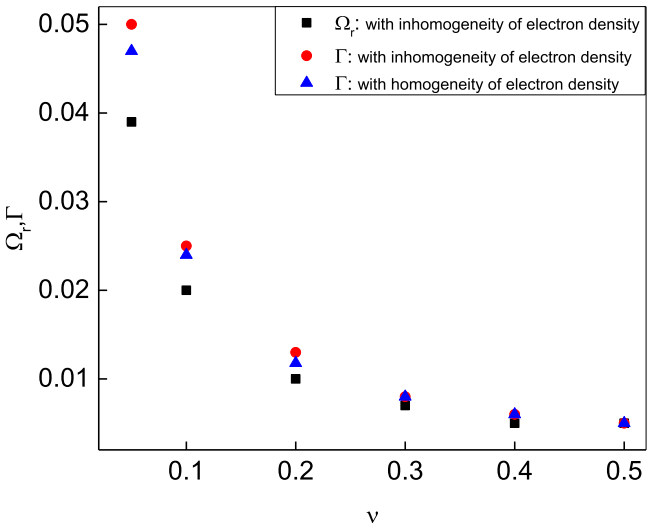


FIG. 3. Real $\Omega_r$ and imaginary $\Gamma$ parts of the frequency for different values of the $\nu$ parameter.

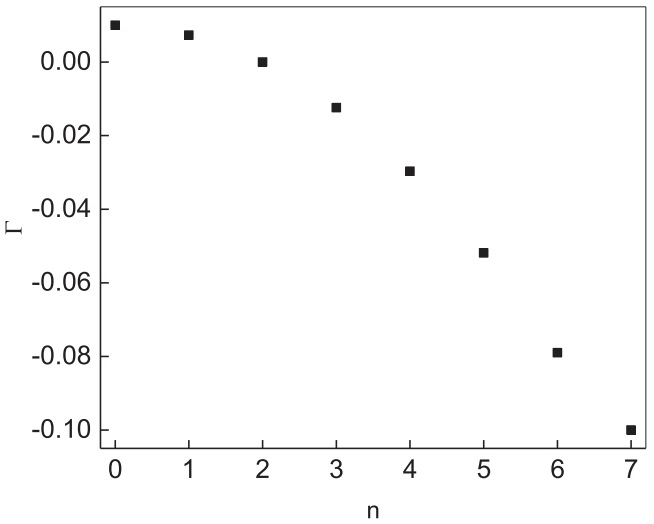


FIG. 4. Imaginary part of the frequency $\Gamma$ for different values of the $n$ parameter.

In other words, collisions cause detuning between the particle density perturbations and the reactive fields which attenuate the current filamentation instability [47]. Comparing results obtained for the inhomogeneous vs homogeneous cases shows that the effect of the electron velocity on the growth rate is similar in both cases. This confirms the results achieved in Ref. [10].

Similar to the procedure presented above, the real and imaginary parts of the frequency can be obtained in the diffusion frequency limit. From Eq. (30), the wave number can be obtained as

$$k_x(\omega,x)=\sqrt{\omega_{p_{e0}}^2\frac{x}{L}\left(\frac{u^2(3q_e-1)}{2v_{T_e}^2}+i\frac{\omega}{\nu_{\rm en}}\right)-\omega_{p_i}^2}. \tag{36}$$

Substituting Eq. (36) into Eq. (31), we have

$$\frac{2L}{c\omega_{p_{e0}}^2\left(\frac{u^2(3q_e-1)}{2v_{T_e}^2}+i\frac{\omega}{\nu_{\rm en}}\right)}\left\{\left[\omega_{p_{e0}}^2\left(\frac{u^2(3q_e-1)}{2v_{T_e}^2}+i\frac{\omega}{\nu_{\rm en}}\right)-\omega_{p_i}^2\right]^{3/2}+i\omega_{p_i}^3\right\}=n\pi. \tag{37}$$

Using the dimensionless parameters, $\nu_{\rm en}/\omega_{p_{e0}}=\nu$, $\omega/\omega_{p_{e0}}=\Omega$, $u/v_{T_e}=U$, $\omega_{p_i}/\omega_{p_{e0}}=\Omega_i$, and $L\omega_{p_{e0}}/c=L'$, Eq. (37) is reduced to

$$\frac{2L'}{\frac{U^2(3q_e-1)}{2}+i\frac{\Omega}{\nu}}\left\{\left[\frac{U^2(3q_e-1)}{2}+i\frac{\Omega}{\nu}-\Omega_i^2\right]^{3/2}+i\Omega_i^3\right\}=n\pi. \tag{38}$$

Similarly to the process presented above, Eq. (38) can be solved using numerical techniques. In Fig. 4, the $\Gamma$ parameter for different values of $n$ is obtained. The parameters used in this figure are $U=0.2$, $\nu=0.1$, $L'=10$, $q_e=2$, and $\Omega_i=0.025$. The real part of the frequency not presented in this figure is 0. One can easily see from this figure that for $n<2$ the plasma system is unstable, while for $n>2$

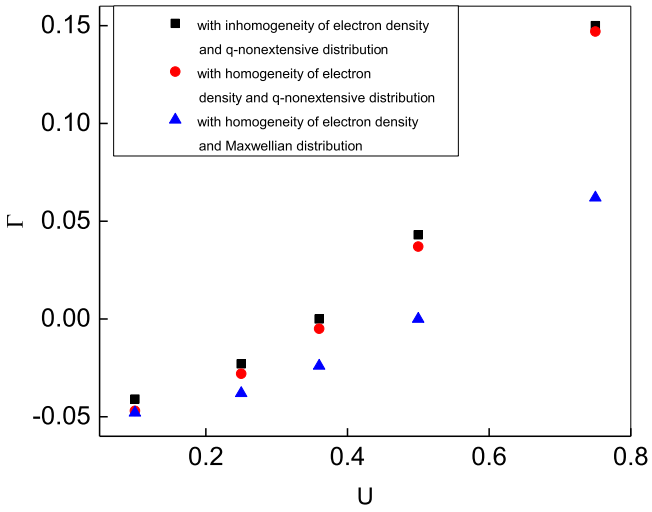


FIG. 5. Imaginary part of the frequency Γ for different values of the $U$ parameter.

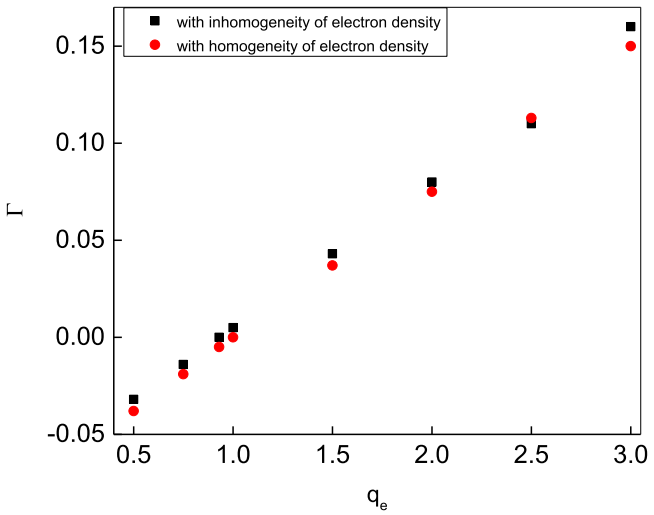


FIG. 6. Imaginary part of the frequency Γ for different values of the $q_e$ parameter.

the imaginary part of the frequency is less than 0, which leads to the stability of the system. In Fig. 5, the effect of the normalized electron velocity on the growth rate of the instability is plotted. The parameters used in this figure are $n = 3$, $\nu = 0.2$, $L' = 10$, $q_e = 1.5$, $\Omega_i = 0.025$, and $k' = 0.5$. For comparison, results are also shown in three cases: in the presence of inhomogeneity of the electron density and $q$-nonextensive electron distribution function, in the presence of homogeneity of the electron density and $q$-nonextensive electron distribution function, and in the presence of homogeneity of the electron density and Maxwellian electron distribution function. It is obvious from this figure that by increasing the normalized electron velocity, the growth rate of instability increases. However, in the presence of inhomogeneity of the electron density and $q$-nonextensive electron distribution function, for electron velocities less than 0.36 the system is stable, while for higher values the plasma system is unstable. In the presence of homogeneity of the electron density and $q$-nonextensive electron distribution function, for electron velocities less than 0.38 (not shown in this figure) the system is stable, while for higher values the plasma system is unstable. In the presence of homogeneity of the electron density and Maxwellian electron distribution function, for electron velocities less than 0.5 (not shown in this figure), the system is stable, while for higher values the plasma system is unstable. The reason for this behavior is as follows: This work presents the current-driven filamentation instability. In a plasma with a current, a magnetic field can be generated around its axis, i.e., $B \approx 4\pi nu/(kc)$. This force can compress the plasma layer. It is concluded from this field that by increasing the electron velocity ($u$ parameter), the generated magnetic field becomes stronger. On the other hand, the electron velocity must be higher than a certain value, which leads to the magnetic pressure becoming higher than the kinetic pressure, and consequently the pinch filaments increase. This leads to an increase in the growth rate of the filamentation instability. Allen *et al.* [48] have shown that the filament size is of the order of the plasma skin depth ($c/\omega_{p_e}$). When the filaments reach the plasma skin depth the instability saturates. At this point the filaments no longer focus, the high space charge and larger emittance dominate, and the filaments first defocus and then merge. Comparing this work and results obtained in Ref. [10] for homogeneous plasma, it is deduced that for homogeneous plasma the instability conditions are $k_0^2 > k^2$ and $u^2(3q_e - 1) > 2v_s^2$ (see Eq. (21) in Ref. [10]), while for inhomogeneous plasma the instability condition is $U > 0.36$. In order to investigate the nonextensive effect on the filamentation instability, in Fig. 6 the growth rate for different values of the $q_e$ parameter is drawn in the presence of inhomogeneity and homogeneity of the electron density. The different parameter used in this figure is $U = 0.5$ and other parameters are similar to those in Fig. 5. It is easy to see in this figure that in the presence of inhomogeneity of the electron density for $q_e < 0.93$, the plasma system is stable, while for values higher than 0.93 the growth rate is greater than 0 and the instability appears. In the presence of homogeneity of the electron density, this condition is $q_e < 1$. However, when the $q_e$ parameter is increased the growth rate of the instability increases. The reason for this behavior is as follows: As we know, when the nonextensive parameter is increased the effective electron temperature decreases. Since the formed filaments can be disturbed by the thermal effects, when the electron temperature is increased the plasma system goes to the stable equilibrium state. This means that at a lower temperature, the plasma tends toward instability. Furthermore, according to Fig. 5 in Ref. [42], when the $q_e$ parameter is increased the electron distribution function becomes wider. This point indicates that the number of energetic electrons which are in the tail of the electron distribution function increases. This is equivalent to electrons with higher values of the electron velocity, and according to Fig. 5 the growth rate of the instability increases. In addition, some authors have investigated the physics of the $q$-nonextensive parameter. Du [49] has shown that the $q$-nonextensive parameter is proportional to the gradient of the temperature. Therefore, $q \neq 1$ is responsible for the spatial inhomogeneity of the temperature as well as the

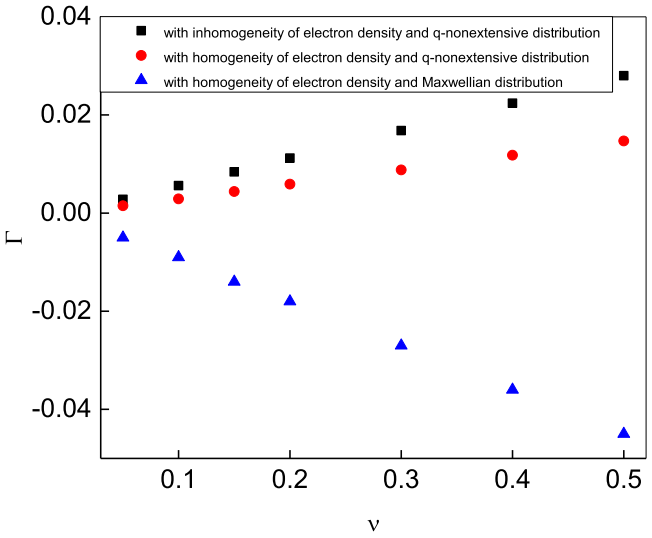


FIG. 7. Imaginary part of the frequency Γ for different values of the $q_e$ parameter.

systems with long-range interactions. However, it is rationally related to the nonisothermal nature of the long-range interaction systems in the nonequilibrium state. Lima *et al.* [43] have shown that the collisional equilibrium is given by the Tsallis $q$-nonextensive velocity distribution. They obtained that when $q < 0$, the entropy of a given volume element decreases with time. Therefore, it is concluded that according to the second law of thermodynamics, the $q$ parameter should be restricted to positive values. Another important point is that if $q = 0$, the entropy of the system does not change with time. Naturally, the $q$-nonextensive parameter may be further restricted by other physical requirements, such as a finite total number of particles. In point of fact, appropriate normalization of the Tsallis distribution requires a $q$ parameter greater than $1/3$. Moreover, using weak-turbulence theory, Yoon *et al.* [50] have shown that the "plasma parameter" $g = 1/(n\lambda_D^3)$, where $\lambda_D = (T_e/(4\pi N_e e^2))^{1/2}$ turns out to play a pivotal role. They found that a small but moderately finite value of $g$ is necessary for a superthermal tail to be generated. Since in the presence of a Tsallis distribution, the $q$-nonextensive parameter is inversely proportional to the effective temperature, it is concluded that the plasma parameter is related to the $q$ parameter. This means that the nonextensive parameter is responsible for the superthermal tail and high-energy particles. However, purely collisionless ($g = 0$) Vlasov theory cannot produce a superthermal population. In Fig. 7, the effect of the normalized collision frequency on the growth rate is shown. In this figure the parameters $U = 0.4$ and $q_e = 1.5$ are used, and the other parameters are similar to those in Fig. 6. For comparison, results are also indicated in three cases: in the presence of inhomogeneity of the electron density and $q$-nonextensive electron distribution function, in the presence of homogeneity of the electron density and $q$-nonextensive electron distribution function, and in the presence of homogeneity of the electron density and Maxwellian electron distribution function. One can see for the $q$-nonextensive electron distribution function that when the normalized collision frequency is increased, the growth rate of the filamentation instability increases, while for the Maxwellian electron distribution function the system is stable. The physical interpretation of the first case can be explained as follows: The collision frequency between electrons and neutrals can decrease the velocity of electrons. Consequently, the number of electrons having enough energy to leave the filaments decreases, which leads to an increase in the instability growth rate. However, for a Maxwellian electron distribution function, the condition presented above is $k_0^2 < k^2$, which leads to stability of the plasma. Finally, it is important to note that according to Eq. (33) or (36) and for a certain value of $x$, $k_x$ becomes 0 or $\infty$. That Eq. (33) can be $\infty$ for $x = -iL\omega\nu_{\rm en}c^2/(u\omega_{p_{e0}})^2$ becomes impossible because $x$ must be real. Equation (36) is 0 for $x = L\omega_{p_i}^2/(\omega_{p_{e0}}^2(u^2(3q_e - 1)/(2v_{T_e}^2) + i\omega/\nu_{\rm en}))$. This value of $x$ is clearly complex. However, for $\nu_{\rm en} = 0$, $k_x$ becomes 0. Since $\nu_{\rm en}$ is not 0, $k_x$ nowhere becomes 0 or $\infty$. Therefore, there are no turning points or clustering points arising in this problem. It is worthwhile to mention some practical values. For example, Allen *et al.* [48] have experimentally studied the current filamentation instability. They have used the electron densities of $1.6 \times 10^{16}$, $1.2 \times 10^{17}$, and $1.9 \times 10^{17}$ cm$^{-3}$. Therefore, in this work we use these numerical values. Considering $N_{e0} = 1.9 \times 10^{17}$ cm$^{-3}$ ($\omega_{p_{e0}} = 2.5 \times 10^{13}$ Hz), the physical parameters are $u = 3.9 \times 10^8$ cm/s ($U = 3$ and $v_{T_e} = 1.3 \times 10^8$ cm/s), $n = 3$, $\nu_{\rm en} = 5 \times 10^{12}$ Hz ($\nu = 0.2$), $L = 1.2 \times 10^{-2}$ cm ($L' = 10$), $q_e = 3$, $\Omega_i = 6.25 \times 10^{11}$ Hz, and $k = 4.2 \times 10^2$ cm$^{-1}$ ($k' = 0.5$). Using these values, the growth rate of the instability is $4 \times 10^{12}$ Hz ($\Gamma = 0.16$).

## V. SUMMARY AND CONCLUSION

In this work, using the $q$-nonextensive electron velocity distribution and linear inhomogeneity of plasma, discrete eigenmodes of the filamentation instability are studied in a weakly ionized current-driven plasma. Considering the moving electrons, immobile ions, and BGK collision model, the generalized longitudinal and transverse dielectric permittivities of collisional current-driven plasmas are obtained. Results are discussed in two limits: long wavelength and diffusion frequency. In the long-wavelength limit, when the $n$ and $U$ parameters are increased $\Omega_r$ increases. Although $\Gamma$ for all $n$ parameters is the same, when the $U$ parameter is increased the growth rate of the instability increases. It is also indicated that when the $\nu$ parameter is increased, the growth rate of the instability decreases. Results of the diffusion frequency limit show that when the $n$ parameter is increased the plasma goes from an unstable mode to a stable one. Moreover, in the presence of inhomogeneity of the electron density and a $q$-nonextensive electron distribution function, for a $U$ parameter less than 0.36 the plasma is stable, while for greater amounts the plasma is unstable. The effect of the $q_e$ parameter on the $\Gamma$ parameter illustrates that the filamentation instability occurs for $q_e > 0.93$ in the presence of a $q$-nonextensive electron distribution function. Although in the long-wavelength limit, the collision frequency decreases the growth rate of the instability, in the diffusion frequency limit and in the presence of a $q$-nonextensive electron distribution function, when the collision frequency is increased the growth rate of the instability increases. However,

in the presence of the Maxwellian electron distribution function, the plasma system is stable. Finally, it is concluded that there are no turning points or clustering points in this problem.

**ACKNOWLEDGMENT**

M.H. thanks Shahrood University of Technology (Grant No. 24051) for their support of the work.

[1] R. D. Jones, W. C. Mead, S. V. Coggeshall, C. H. Aldrich, J. L. Norton, G. D. Pollak, and J. M. Wallace, Phys. Fluids **31**, 1249 (1988).
[2] K. A. Tanaka, M. M. Allen, A. Pukhov, R. Kodama, H. Fujita, Y. Kato, T. Kawasaki, Y. Kitagawa, K. Mima, N. Morio, H. Shiraga, M. Iwata, T. Miyakoshi, and T. Yamanaka, Phys. Rev. E **62**, 2672 (2000).
[3] X. P. Xia, Z. B. Cai, and L. Yi, Laser Part. Beams **29**, 161 (2011).
[4] A. J. Schmitt and B. B. Afeyan, Phys. Plasmas **5**, 503 (1998).
[5] C. M. Huntington, A. G. R. Thomas, C. McGuffey, T. Matsuoka, V. Chvykov, G. Kalintchenko, S. Kneip, Z. Najmudin, C. Palmer, V. Yanovsky, A. Maksimchuk, R. P. Drake, T. Katsouleas, and K. Krushelnick, Phys. Rev. Lett. **106**, 105001 (2011).
[6] L. Vlahos, Adv. Space Res. **13**, 161 (1993).
[7] D. Caprioli and A. Spitkovsky, Astrophys. J. Lett. **765**, L20 (2013).
[8] C. Shukla, A. Das, and K. Patel, Phys. Plasmas **22**, 112118 (2015).
[9] A. F. Alexandrov, L. S. Bogdankevich, and A. A. Rukhadze, *Principles of Plasma Electrodynamics* (Springer, Berlin, 1984).
[10] S. M. Khorashadizadeh, E. Rastbood, and A. R. Niknam, Phys. Plasmas **22**, 072103 (2015).
[11] Y. M. Aliev, V. Y. Bychenko, and A. A. Frolov, Plasma Phys. **25**, 827 (1983).
[12] F. Califano, R. Prandi, F. Pegoraro, and S. V. Bulanov, Phys. Rev. E **58**, 7837 (1998).
[13] M. Honda, Phys. Rev. E **69**, 016401 (2004).
[14] B. Mohammadhosseini, A. R. Niknam, and B. Shokri, Phys. Plasmas **17**, 122303 (2010).
[15] A. Renyi, Acta Math. Acad. Sci. Hungarica **6**, 285 (1955).
[16] C. Tsallis, J. Stat. Phys. **52**, 479 (1988).
[17] J. R. Asbridge, S. J. Bame, and I. B. Strong, J. Geophys. Res. **73**, 5777 (1968).
[18] R. Lundin, A. Zakharov, R. Pellinen, H. Borg, B. Hultqvist, N. Pissarenko, E. M. Dubinin, S. W. Barabash, I. Liede, and H. Koskinen, Nature **341**, 609 (1989).
[19] Y. Futaana, S. Machida, Y. Saito, A. Matsuoka, and H. Hayakawa, J. Geophys. Res. **108**, 151 (2003).
[20] N. Divine and H. B. Garret, J. Geophys. Res. **88**, 6889 (1983).
[21] S. M. Krimigis, J. F. Carbary, E. P. Keath, T. P. Armstrong, L. J. Lanzerotti, and G. Gloeckler, J. Geophys. Res. **88**, 8871 (1983).
[22] W. M. Moslem, R. Sabry, S. K. El-Labany, and P. K. Shukla, Phys. Rev. E **84**, 066402 (2011).
[23] J. M. Liu, J. S. De Groot, J. P. Matte, T. W. Johnston, and R. P. Drake, Phys. Rev. Lett. **72**, 2717 (1994).
[24] C. Tsallis and A. M. C. de Souza, Phys. Lett. A **235**, 444 (1997).
[25] Z. Voros, Ann. Geophys. **18**, 1273 (2000).
[26] Z. Voros, W. Baumjohann, R. Nakamura, A. Runov, T. L. Zhang, M. Volwerk, H. U. Eichelberger, A. Balogh, T. S. Horbury, K.-H. Glameier, B. Klecker, and H. Reme, Ann. Geophys. **21**, 1995 (2003).
[27] Z. Voros, W. Baumjohann, R. Nakamura, M. Volwerk, A. Runov, T. L. Zhang, H. U. Eichelberger, R. Treumann, E. Georgescu, A. Balogh, B. Klecker, and H. Reme, J. Geophys. Res. **109**, A11215 (2004).
[28] M. P. Leubner and Z. Voros, Astrophys. J. **618**, 547 (2005).
[29] M. P. Leubner and Z. Voros, Nonlin. Proc. Geophys. **12**, 171 (2005).
[30] G. P. Pavlos, M. N. Xenakis, L. P. Karakatsanis, A. C. Iliopoulos, A. E. G. Pavlos, and D. V. Sarafopoulos, Phys. A **395**, 58 (2014).
[31] J. A. S. Lima, R. Silva Jr., and J. Santos, Phys. Rev. E **61**, 3260 (2000).
[32] H. B. Qiu and S. B. Liu, Phys. Plasmas **20**, 102119 (2013).
[33] S. M. Khorashadizadeh, E. Rastbood, and A. R. Niknam, Phys. Plasmas **21**, 122106 (2014).
[34] A. R. Niknam, E. Rastbood, S. M. Khorashadizadeh, and A. Entezari Roodbaraki, Astrophys. Space Sci. **357**, 50 (2015).
[35] M. Hashemzadeh, Physica A (Amsterdam) **459**, 68 (2016).
[36] H. Lashinsky, Phys. Rev. Lett. **12**, 121 (1964).
[37] M. N. Rosenbluth, Phys. Rev. Lett. **29**, 565 (1972).
[38] S. M. Grach, A. N. Karashtin, N. A. Mitiakov, V. O. Rapoport, and V. Iu. Trakhtengerts, Fiz. Plaz. **4**, 1330 (1978) [Sov. J. Plasma Phys. **4**, 742 (1978)].
[39] X. Xiongping and Y. Lin, Plasma Sci. Technol. **14**, 1054 (2012).
[40] L. J. Guo, L. X. Guo, and J. T. Li, Phys. Plasmas **24**, 022108 (2017).
[41] A. Ramani and C. E. Max, Phys. Fluids **26**, 1079 (1983).
[42] A. R. Niknam, H. Roozbahani, M. Hashemzadeh, and D. Komaizi, Phys. Plasmas **21**, 092307 (2014).
[43] J. A. S. Lima, R. Silva, and A. R. Plastino, Phys. Rev. Lett. **86**, 2938 (2001).
[44] J. A. Davies, M. Lester, and T. R. Robinson, Ann. Geophys. **15**, 1557 (1997).
[45] J. R. Roth, *Industrial Plasma Engineering: Vol. 2. Application to Nonthermal Plasma Processing* (Institute of Physics, Philadelphia, 2001).
[46] B. Hao, Z.-M. Sheng, and J. Zhang, Phys. Plasmas **15**, 082112 (2008).
[47] B. Hao, Z.-M. Sheng, C. Ren, and J. Zhang, Phys. Rev. E **79**, 046409 (2009).
[48] B. Allen, V. Yakimenko, M. Babzien, M. Fedurin, K. Kusche, and P. Muggli, Phys. Rev. Lett. **109**, 185007 (2012).
[49] J. Du, Europhys. Lett. **67**, 893 (2004).
[50] P. H. Yoon, T. Rhee, and C.-M. Ryu, Phys. Rev. Lett. **95**, 215003 (2005).